

Effect of the shaft eccentricity on the hydrodynamics of unbaffled stirred tanks

G. Montante^{a,*}, A. Bakker^b, A. Paglianti^a, F. Magelli^a

^a*Dipartimento di Ingegneria Chimica, Mineraria e delle Tecnologie Ambientali, Università di Bologna - Viale Risorgimento 2-40136, Bologna, Italy*

^b*Fluent Inc., Lebanon, NH 03766, USA*

Received 19 July 2005; received in revised form 15 September 2005; accepted 23 September 2005

Available online 9 January 2006

Abstract

The aim of this work is to investigate the effect of the shaft eccentricity on the hydrodynamics of unbaffled stirred vessels. The difference between coaxial and eccentric agitation is studied using a combination of experiments carried out by particle image velocimetry, that provide an accurate representation of the time-averaged velocity, and computational fluid dynamics simulations, that offer a complete, transient volumetric representation of the three-dimensional flow field, once a proper modelling strategy is devised. The comparison of the experimental and simulated mean flow fields has demonstrated that calculations based on Reynolds-averaged Navier–Stokes equations are suitable for obtaining accurate results. Depending on the position of the shaft, steady-state or transient calculations have to be chosen for predicting the correct flow patterns. Care must be exerted in the choice of turbulence models, as for the unbaffled configurations the results obtained with the Reynolds stress model are superior to that of the $k-\epsilon$ model.

© 2005 Elsevier Ltd. All rights reserved.

Keywords: Fluid mechanics; Hydrodynamics; Mixing; Simulation; Eccentric agitation; Unbaffled vessel; PIV

1. Introduction

Nowadays, computational fluid dynamics (CFD) simulations based on the solution of Reynolds-averaged Navier–Stokes equations (RANS) are feasible tools for design and optimisation of several apparatuses of chemical and process industry (Joshi and Ranade, 2003, Bakker et al., 1994a,b). In the past decade, many efforts have been devoted to the development of mathematical models for CFD and the capabilities of the models in predicting equipment fluid dynamics have often been assessed through the comparison with experimental data. After many years of investigations, the potential of RANS calculations to simulate the flow field in stirred vessels have been widely inspected: satisfactory predictions of the mean flow field of single-phase, baffled stirred tanks have been obtained (Brucato et al., 1998), while poor results are often achieved for the turbulent characteristics of the flow (Ng and

Yianneskis, 2000). In the earlier studies, the simulations of baffled stirred vessels were performed using “black box” methods, that require experimental data as boundary conditions (e.g. Ranade et al., 1989). The successful development of appropriate fully predictive strategies, as reviewed by Brucato et al. (1998), has allowed to overcome the need of preliminary experimentation and has opened the way for the adoption of CFD for the selection and the design of stirred vessels. For the simulation of single-phase baffled stirred vessels, the more appropriate mathematical models and computational strategy to adopt when using RANS-based CFD codes is presently fairly well known. From a geometrical point of view, the unbaffled vessels are simpler than the baffled ones. Therefore, it could be presumed that reliable forecasts of the fluid dynamics of such apparatuses are obtainable just by solving the same mathematical models that were proved to be suitable for baffled vessels, but without the need of resorting to particular simulation strategies, thus reducing the computational cost and complexity. However, previous works have already assessed that the simulation of unbaffled stirred tanks is not an easy task (Armenante et al., 1997; Ciofalo et al., 1996). Nevertheless,

* Corresponding author. Tel.: +39 051 2090406; fax: +39 051 6347788.
E-mail address: giusi.montante@mail.ing.unibo.it (G. Montante).

the unbaffled stirred tank configuration has been adopted as a test case for two-equation turbulence models instead of the baffled case due to the geometrical simplicity (Jones et al., 2001) and treated in the same way as baffled tanks (Murthy and Jayanti, 2002). A review on the modelling of unbaffled stirred vessels can be found in Alcamo et al. (2005), who performed large eddy simulations (LES) of an unbaffled stirred vessel provided with a coaxial impeller and obtained satisfactory results in terms of both mean and turbulent characteristics of the flow. Generally, scarce information concerning unbaffled stirred vessels provided with coaxial mixers is available, although unbaffled vessels are sometimes used in industrial practice, e.g. when fouling on the vessel internals is to be limited or for mixing of very viscous materials (Novak and Rieger, 1994). Eccentric configurations have been even less studied, but probably they have a wider practical interest, as the off-centre impeller positioning improves the mixing performance with respect to that of centred impellers (Hall et al., 2004) while being featured by smaller surface vortexing. The effect of impeller eccentricity on mixing has been experimentally investigated in a few works (e.g. Nishikawa et al., 1979; Medek and Fort, 1985; Karcz et al., 2005; Hall et al., 2005), but knowledge on these systems is still rather incomplete. For the laminar regime, the effect of the shaft position on the flow field has been experimentally investigated by Alvarez et al. (2002), who found important changes in the flow structure and major enhancement in mixing behaviour even for low eccentricity conditions. On the computational side, Rivera et al. (2004) have already pointed out that off-centred impellers pose particular simulation difficulties. They performed the simulations of eccentric mixer configurations in laminar regime, while to the best of our knowledge validated simulations of eccentric stirred vessels in the turbulent flow regime have not been published in the open literature to date.

In this work the hydrodynamics of an unbaffled vessel, stirred with a Rushton turbine located either coaxially or eccentrically are investigated by particle image velocimetry (PIV). The particular flow features of the eccentric configuration are further investigated by RANS-based CFD simulations. The comparison of the results with the experiments has confirmed that unsteady RANS (URANS) simulations predict correctly the mean flow field in off-centre stirred vessels. In this case, the proper simulation strategy differs from that commonly adopted for baffled stirred vessels as well as from that devised for unbaffled vessels stirred coaxially.

2. Experimental

The investigation was carried out in a cylindrical tank (tank diameter, $T = 23.6$ cm, tank height, $H = T$), made of Perspex, provided with a flat base and a lid on the top. Agitation was provided with a standard six bladed Rushton turbine (RT) of diameter $D = T/3$ placed at the distance $C = T/2$ from the vessel base (Fig. 1a). For the eccentric configuration, the shaft was located at 58 mm ($E = T/4$) from the vessel axis (Fig. 1b). The shaft and impeller were painted matt black to minimise light reflection. The vessel was contained inside a trough filled with the working liquid, that was water at room temperature, in order to reduce the laser light refractive effects at the curved tank surface. The impeller rotational speed was fixed at 400 rpm, corresponding to a velocity of the blade tip, V_{tip} , equal to 1.65 m/s, and producing an impeller Reynolds number, Re , equal to 4.1×10^4 .

The measurements were performed using a Dantec Dynamics PIV system. The laser sheet source adopted was a pulsed Nd:YAG laser, emitting light at 532 nm with a maximum frequency of 15 Hz. The image capturing was performed

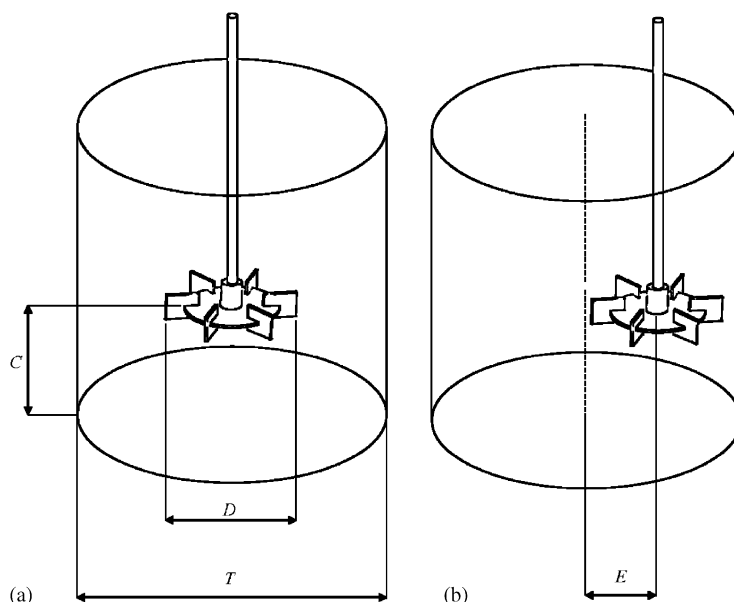


Fig. 1. Geometrical configurations of the stirred vessel. (a) coaxial shaft; (b) eccentric shaft.

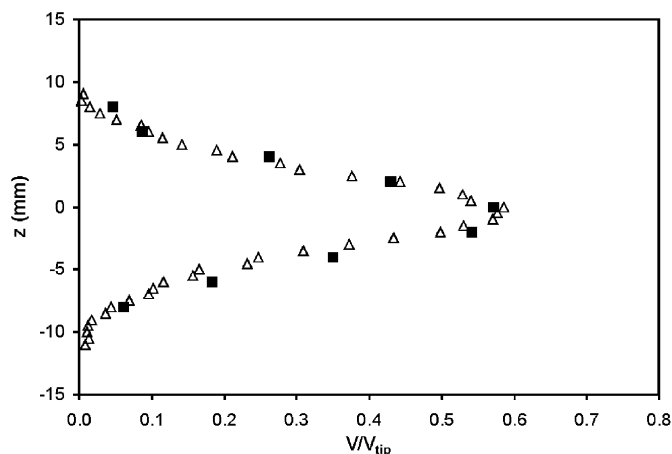


Fig. 2. Comparison of PIV (solid symbols) and LDA (open symbols) axial profile of mean radial velocity normalised with V_{tip} , determined at the radial position of 1.5 mm off the impeller blade.

by a Dantec PCO Camera with a 1280×1024 pixel CCD, cooled by a Peltier module to improve the signal-to-noise ratio. The laser control, the laser/camera synchronisation and the data acquisition and processing were handled by a hardware module (FlowMap System Hub) and FlowManager software installed on a PC. The liquid was seeded with silver-coated hollow glass particles of mean diameter equal to $10 \mu\text{m}$. The seeding particles concentration was carefully chosen in order to obtain from 5 to 10 particles for each interrogation area. The measurements were performed in several horizontal and vertical planes and in each case 300 images were found to be sufficient for obtaining the time averaged flow field. The cross-correlation of the image pairs was performed on a rectangular grid with 50% overlap between adjacent cells; the interrogation area was set at 32×32 pixel and each image contained the whole horizontal or vertical vessel section. Particular care was used to eliminate measuring error sources. For instance, the average pixel intensity was subtracted from each single image pair for reducing noise and the velocity vectors of magnitude bigger than V_{tip} were discarded. The vessel was closed with a lid on the top, in order to avoid uncertainties in the velocity measurements due to air bubbles entrainment.

Preliminary measurements were performed in order to assess the PIV set-up and data processing procedure. To this end the vessel described above was provided with removable baffles and coaxial stirrer and the measured mean velocities were compared with the corresponding LDA data collected by Brunazzi et al. (2003) in the same vessel and with the same turbine. The accuracy of the PIV data was found to be sufficiently high, as can be observed in Fig. 2, where the two mean radial velocity profiles normalised with V_{tip} are shown.

3. CFD simulations

The simulations were performed running the finite volume general purpose CFD code FLUENT 6.2. The computational grid, that was refined in the region containing the impeller

blades, where the biggest velocity gradients were expected, consisted of a total of about 314,000 hexahedral cells over a domain of 2π . A specific grid independency study was not performed on the basis of previous experience on stirred vessel simulations, suggesting that the present grid was fine enough for obtaining accurate result (e.g. Oshinowo et al., 2000; Montante et al., 2001; Aubin et al., 2004). Wall boundary conditions with conventional “wall-functions” were adopted on the vessel bottom, the lateral wall and the top. A special treatment of the water surface, such as that devised in Ciofalo et al. (1996) was not required, as the vessel was provided with a lid. This choice was made in order to avoid measurement errors and allowed us to separate experimental uncertainties from modelling problems. The RANS equations coupled with the standard $k-\varepsilon$ turbulence model or the Reynolds stress model (RSM), as implemented in the code, were numerically solved in a Cartesian coordinate system. The rotating reference frame where the agitator is steady was chosen for the inner part of the domain, containing the impeller, while a steady reference frame was used for the rest of the vessel. The steady-state multiple reference frame (MRF) approach or the unsteady sliding mesh (SM) approach were adopted. For the MRF and the SM simulations, the extension of the internal and the external domains was identical. The vertical extension of the rotating region was limited to the impeller vicinity—to about 2.5 times the blade height—for avoiding problems of artificial swirl (Oshinowo et al., 2000), while the diameter, imposed by the narrow space between the impeller and vessel wall, was taken equal to $1.25D$. For the transient SM simulation, 329 impeller revolutions with 120 time steps per revolution have been run that correspond to about 50 s of real time. The solution convergence was carefully checked by monitoring the residuals of all variables as well as physical values of the swirl velocity. Residuals were dropped to the order of 10^{-4} or less, which is at least one order of magnitude tighter than Fluent’s default criteria. About 120 revolutions were necessary in order to obtain a fully developed flow field and further 80 revolutions were run to obtain a refined solution based on time monitoring of the volume-averaged tangential velocity as well as on the residuals value. After obtaining a fully developed flow field, 129 more impeller revolutions were calculated and the results were time averaged for performing a consistent comparison with the PIV data.

4. Results and discussion

4.1. PIV results

The agitation provided by the coaxial RT in the unbaffled tank described above gives rise to a mean flow field dominated by the tangential component of the velocity vector in the whole vessel volume. As an example, the velocity vector plots in two horizontal planes, one 60 mm above and the other 60 mm below the impeller disk plane, are shown in Figs. 3(a) and (b), respectively. In this case, the azimuthal extension of the measured vector plots is limited to 90° due to the spatial periodicity of the flow. As can be observed, both the velocity vector plots

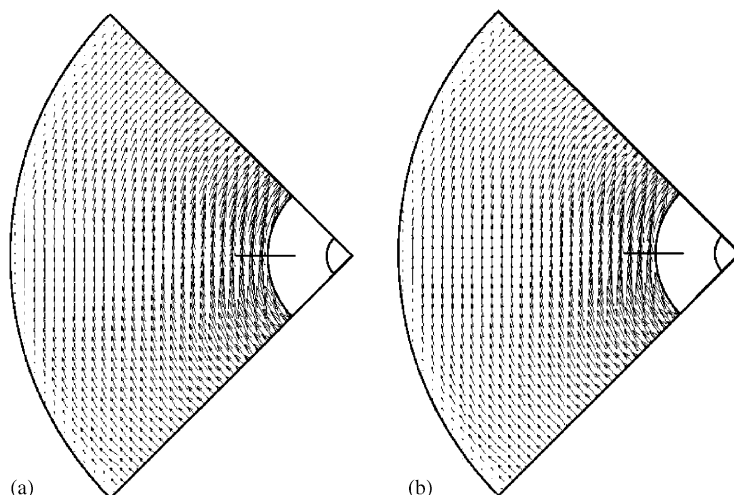


Fig. 3. PIV vector plot for the co-axial configuration: (a) horizontal plane 60 mm above the impeller disk; (b) horizontal plane 60 mm below the impeller disk.

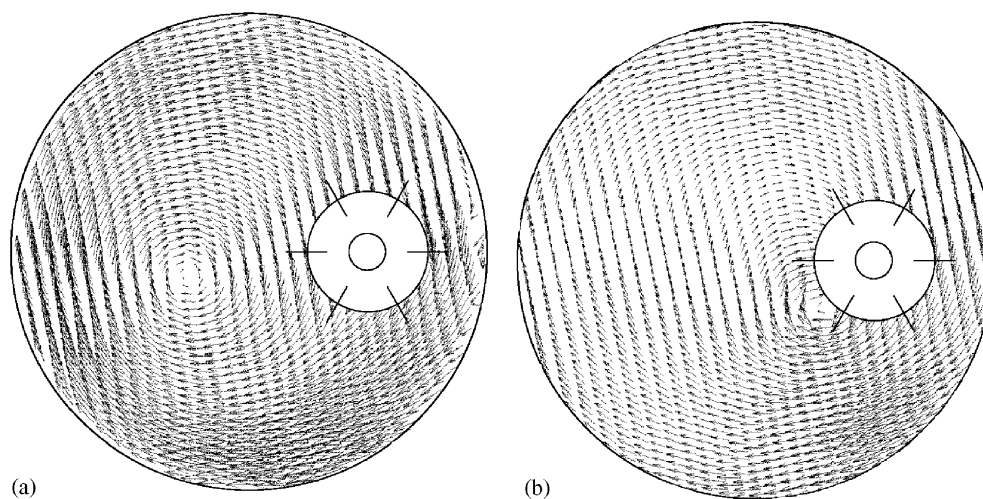


Fig. 4. PIV vector plot for the eccentric configuration: (a) horizontal plane 60 mm above the impeller disk; (b) horizontal plane 60 mm below the impeller disk.

reveal the expected swirl-dominated flow and marked differences between them are not apparent, thus confirming that the liquid is mainly moved along circumferential patterns in the whole vessel volume and that the flow is characterised by important streamline curvature and strong rotation. The horizontal vector plots, relevant to the coaxial configuration at the same elevations selected for the coaxial stirred, are shown in Figs. 4(a) and (b). As can be observed, the flow field is characterised by a different structure: together with a prevailing tangential flow, a vortex located at a distinct position for each elevation can be clearly identified. Overall, the horizontal vector plots obtained at different elevations from the bottom to the vessel top show that there are two vortices, one departing from the impeller and going toward the bottom with an inclination of about 10° from the vertical axis and the other going toward the top and inclined of about 30° . A quantitative estimation of the spatial position of the two vortices is shown in Fig. 5, where the location of each vortex centre at different horizontal vessel sections, as revealed by the PIV vector plots, can be observed

and the difference between the lower and upper vortex pattern can also be appreciated. As the lower and the upper half of the vessel are geometrically identical, the lack of vertical symmetry exhibited by the two vortices can be attributed to the fact that the shaft doesn't extend below the impeller.

The mean velocity field produced by the turbine in the two configurations in a vertical plane containing the agitator and the shaft is shown in Fig. 6. In these plots there are areas without vectors due to optical blockage: in particular, the velocity could not be measured close to the vessel top because of an upper flange and in a small circular region close to the bottom for the presence of the drainage tube of the trough. As can be observed in Fig. 6(a), for the coaxial configuration the typical double loop flow structure is apparent. Apart from maintaining approximately the same qualitative structure of that relevant to a "standard" fully baffled stirred vessel, the vertical flow field in the unbaffled tank stirred with a coaxial impeller presents smaller radial and axial velocity components. Indeed, the measured impeller flow number was found to be equal to 0.25, that

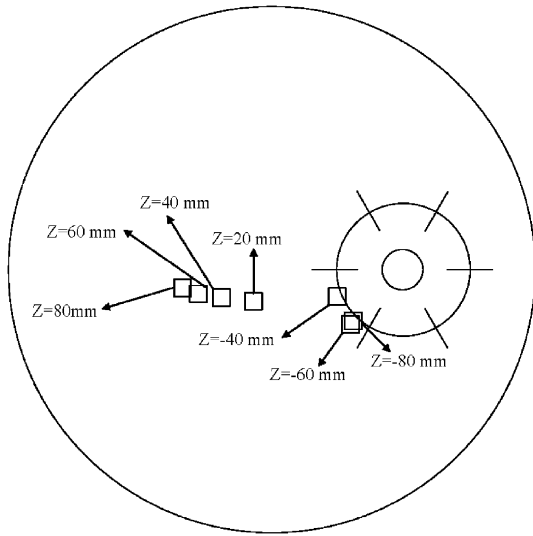


Fig. 5. Location of the main vortex core at different elevations relative to the impeller disk.

is about 65% smaller than the value for the same impeller in baffled vessels. This result is in agreement with that obtained by Brunazzi et al. (2003) from LDA measurements. The significant modification of the flow field structure due to eccentric agitation, already revealed by the measurements in the horizontal planes, is clearly visible also in the vertical vector plot shown in Fig. 6(b) apart from the region at the back of the shaft due to the optical blockage of the laser light. Definitely, the axial symmetry of the flow field is lost, the radial and axial velocity components give rise to an overall elliptic vertical motion and the double loop flow structure generated in coaxial configurations is destroyed.

4.2. CFD results and comparison with experiments

The MRF/RANS simulations of the unbaffled vessel provided with the coaxial stirrer confirmed that the $k-\epsilon$ turbulence model is inappropriate. Indeed, as already shown by Ciofalo et al. (1996), once the RANS equation closure

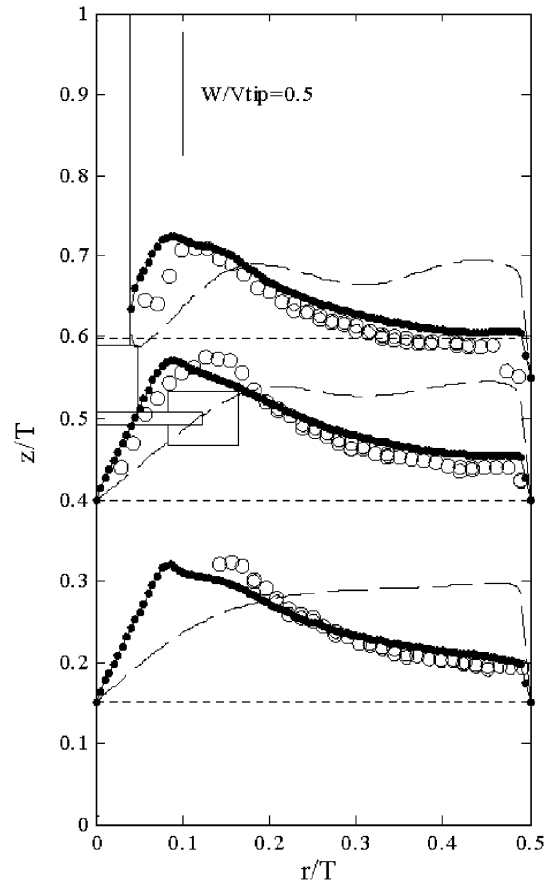


Fig. 7. Comparison of normalised radial profiles of tangential velocity at three different elevations; steady-state simulations of the co-axial vessel. Experimental data: open circles; $k-\epsilon$ simulation: thin dashed lines; RSM simulation: dotted lines and solid symbols.

is performed with the $k-\epsilon$ turbulence model equations, the calculated mean flow field is characterised by an unphysical rigid body rotation and none of the three components of the velocity vector on the vessel volume is realistically predictable. The adoption of the more

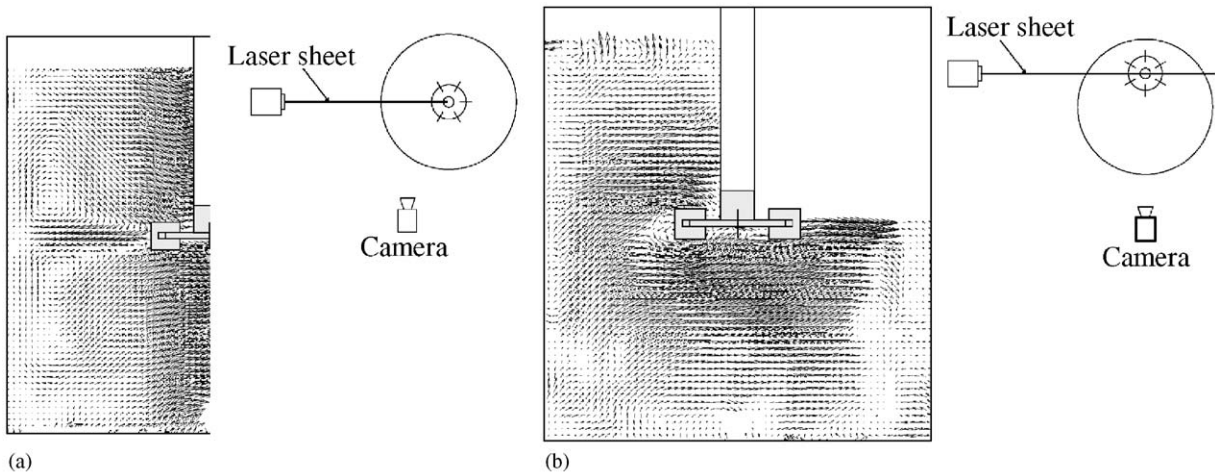


Fig. 6. PIV vector plot in a vertical plane containing the shaft and the impeller: (a) coaxial configuration; (b) eccentric configuration.

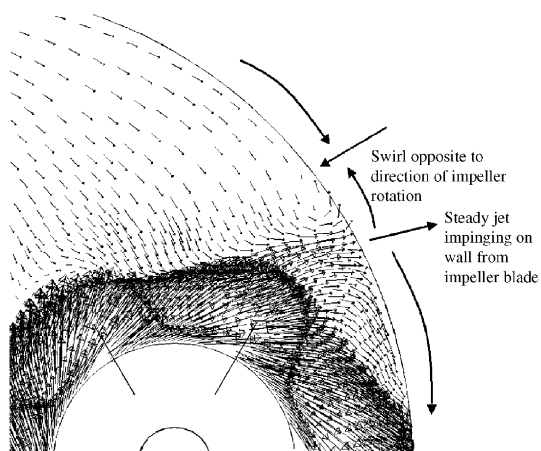


Fig. 8. Velocity vectors in the impeller plane for steady-state simulations using the MRF model and the Reynolds stress turbulence model. The impeller rotates clock-wise. This steady-state model predicts a region of unphysical opposite swirl.

advanced RSM, which is more suited for the anisotropic turbulence in swirling flows, significantly improves the results and acceptable agreement between the experimental and the simulated mean flow field is achieved. The results obtained in this work for the coaxial configuration are not extensively reported for the sake of brevity. As an example of the results quality, the experimental and computed radial profiles of tangential mean velocity at three different elevations are shown in Fig. 7. As can be observed, the $k-\epsilon$ model predictions are definitely unsatisfactory, while the RSM results are physically consistent and quantitatively acceptable for the coaxial stirrer.

Initially, simulations of the eccentricly agitated stirred vessel have been performed using the MRF model and solving the steady state RANS equations coupled with the $k-\epsilon$ model or the RSM. In both cases the flow features were not predicted successfully. In particular, together with the tendency of the liquid to follow a solid body rotation in the $k-\epsilon$ simulation, the complete absence of the vortices shown in the experimental flow pattern resulted with both turbulence models.

Fig. 8 shows a flow detail near the impeller, as predicted using MRF and RSM. As can be observed, the adoption of this approach produces a steady jet that emanates from the impeller blade and impinges on the vessel wall at a fixed location. The jet splits where it impinges on the wall, resulting in a region where the model predicts a flow direction opposite to the rotation of the impeller. This result is not consistent with the experimental flow structure. In actuality, the impeller blade rotates and, instead of impinging steadily on the wall at a fixed location, the jet sweeps along the vessel wall the flow being in the same direction of the impeller rotation in all locations. This dynamic phenomenon is absent in the results from the MRF model, and can only be modelled correctly by using the transient SM approach. Therefore, proper modelling of these transient effects as the impeller blades sweep by the section closest to the vessel wall is crucial to obtain accurate flow field predictions for the eccentric vessel.

The fully time dependent URANS equations coupled with the RSM were, therefore, solved using the SM model. In Figs. 9(a) and (b) the velocity vector plots in the horizontal plane located at 80 mm above the impeller obtained from the PIV measurements and the CFD simulation respectively are shown. The comparison of the two vector plots highlights that the flow structure obtained by means of the PIV measurements is rightly predicted with the simulation and the vortex presence is correctly reproduced and located. The quality of the predicted flow field can be evaluated also from the analysis of the results on the vertical planes, an example of which is provided in Fig. 10: the overall agreement of the experimental (Fig. 10a) and the simulated (Fig. 10b) flow field is apparent.

A quantitative estimation of the simulation accuracy has been performed by comparing the experimental and computed distance of the vortex centre from the shaft axis at different elevations. For a single elevation, the experimental vortex core position has been evaluated in three different sets of data, in order to estimate the measurement accuracy, that was found of 3 mm. The fair agreement of the

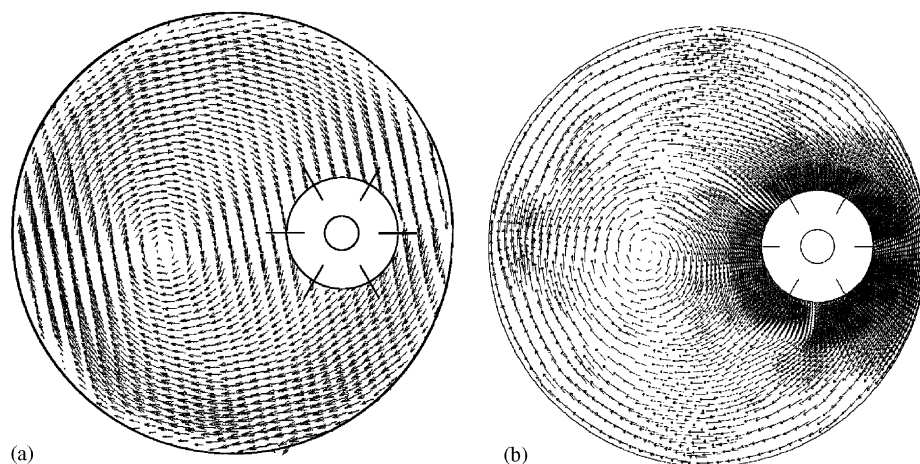


Fig. 9. Vector plot in the horizontal plane 80 mm above the impeller disk for the eccentric configuration: (a) PIV measurements; (b) CFD simulation (SM/RSM simulation).

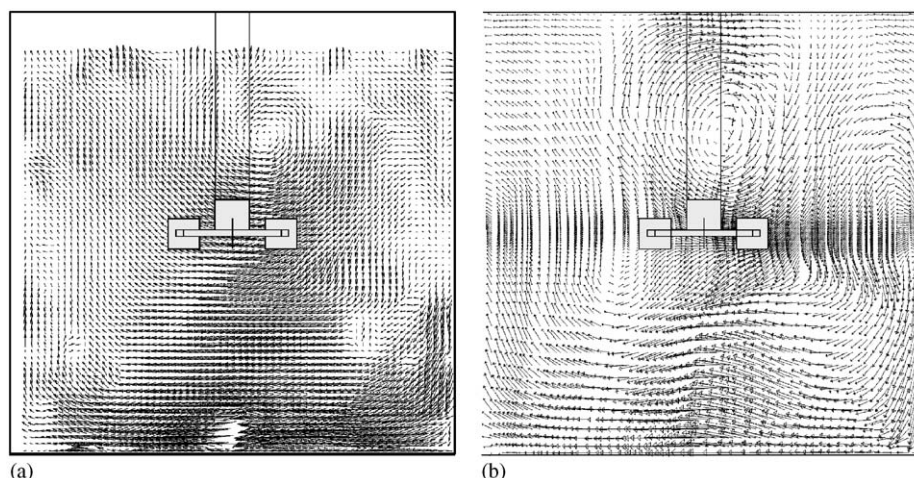


Fig. 10. Vector plot in the vertical plane 80 mm from the impeller axis for the eccentric configuration: (a) PIV measurements; (b) CFD simulation (SM/RSM simulation).

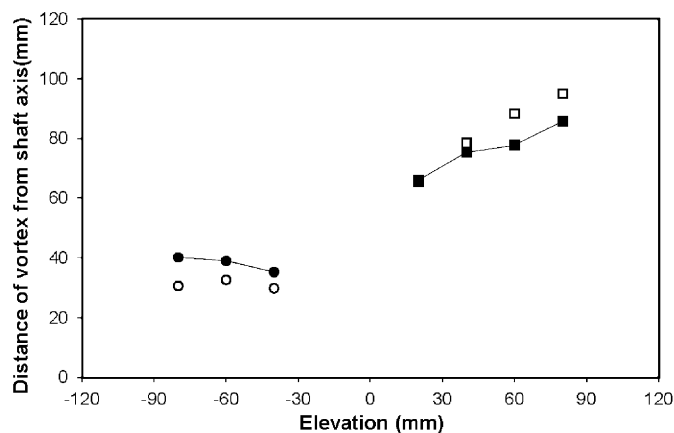


Fig. 11. Distance of the vortex core from the shaft axis at different elevations. Open symbols: PIV results. Solid symbols and lines: CFD results.

results shown in Fig. 11 proves that the selected computational approach is able to provide accurate results.

As a difference with the steady-state simulations, that are appropriate when the flow in the vicinity of the impeller is unaffected by the rest of the tank (Aubin et al., 2004), the transient approach allows to correctly predict the flow field also for stirred vessel configurations characterised by a close interaction between the impeller jet and the vessel wall. The intensity of such interaction, that is related to the impeller jet strength and the distance between the blade tip and the wall, marks the boundary between the reliable applicability of MRF and its failure. Unfortunately, the dimensionless circumferential jet strength varies with the vessel diameter and the impeller Reynolds number also for fully turbulent conditions up to very high values of Re , as shown by Yoon et al. (2005), so that simple, general rules cannot be given. It is, finally, worth noting that the range of applicability of steady RANS method

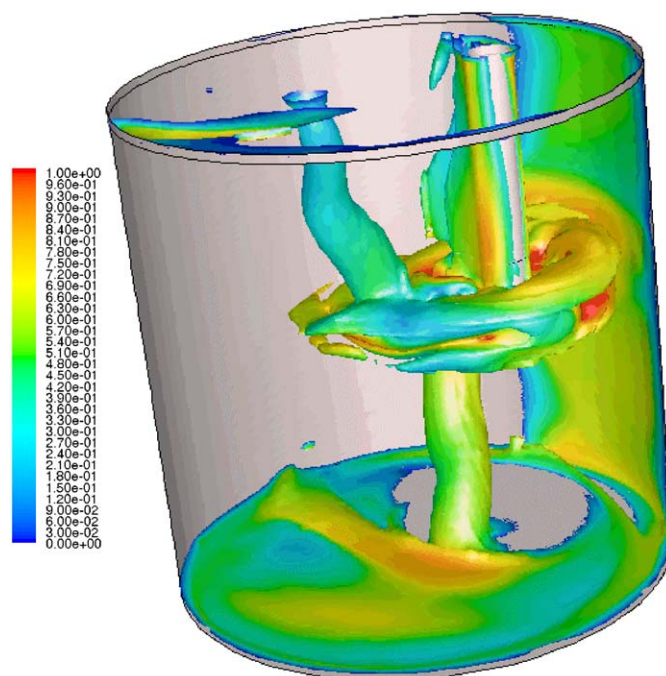


Fig. 12. Iso-surface of vorticity magnitude coloured by velocity magnitude (m/s) (SM/RSM simulation).

cannot be easily identified with a single parameter, e.g. the eccentricity.

Among the advantages of CFD simulations, the availability of a fully transient volumetric representation of the three-dimensional flow field has to be mentioned, as it provides an important contribution to the understanding of the hydrodynamics of stirred vessels. As an example, in the particular case of the eccentric configuration of our unbaffled stirred vessel, the CFD results offer an effective representation of the two vortices by the iso-surface of the vorticity magnitude. It indicates the extent of rotation in the flow and is commonly used

to visualise vortex structures, as can be observed in Fig. 12 that clearly allows us to identify and track the vortices.

5. Conclusion

In this work the effect of the shaft position on the hydrodynamics of unbaffled stirred tanks has been investigated. To this end, measurements of the velocity vectors have been performed in horizontal and vertical planes through the PIV technique. The experiments have revealed some expected features of the coaxial configuration as well as particular characteristics of the eccentric system. The experimental mean flow fields have been also adopted for assessing the possibility to perform reliable RANS-based CFD simulations. The results have led to the conclusion that for the closure of RANS-based simulations satisfactory results can be obtained in some cases with advanced turbulent models, such the RSM, without resorting to much more computationally expensive methods, like LES. Certainly, this consideration holds true once a deep knowledge of mean flow field can be sufficient and very accurate prediction of the turbulent characteristics of the flow are not critically important. The use of RSM is especially important in flow systems characterised by strong anisotropic turbulence, as in the case of unbaffled vessels (Brunazzi et al., 2005), as well as in the case of strong streamline curvature (Wegner et al., 2004).

Steady-state approximations should be avoided whenever the interactions between the impeller jet and a stationary wall are significant. As a difference with other geometrical configurations of stirred vessels, in the particular case of the present eccentric geometry, the adoption of transient calculations is required in order to reproduce the complex features of the flow patterns.

Acknowledgements

This work was financially supported by Italian Ministry of University and Education (FIRB 2001 project). The collaboration of Ing. Alessandro Angelini in carrying out the experimental programme and of Dr. Germano Ragosta (FluxOptica) for the support on the PIV set-up are gratefully acknowledged.

References

- Alcamo, R., Micale, G., Grisafi, F., Brucato, A., Ciofalo, M., 2005. Large-eddy simulation of turbulent flow in an unbaffled stirred tank driven by a Rushton turbine. *Chemical Engineering Science* 60, 2303–2316.
- Alvarez, M.M., Arratia, P.E., Muzzio, F.J., 2002. Laminar mixing in eccentric stirred tank systems. *Canadian Journal of Chemical Engineering* 80, 546–557.
- Armenante, P.M., Luo, C., Chou, C., Fort, I., Medek, J., 1997. Velocity profiles in a closed unbaffled vessel: comparison between experimental LDV data and numerical CFD predictions. *Chemical Engineering Science* 20, 3483–3492.
- Aubin, J., Fletcher, D.F., Xuereb, C., 2004. Modeling turbulent flow in stirred tanks with CFD: the influence of the modelling approach, turbulence model and numerical scheme. *Experimental Thermal and Fluid Science* 28, 431–445.
- Bakker, A., Morton, J.R., Berg, G.M., 1994a. Computerising the steps of mixer selection. *Chemical Engineering*, 101, 120–129.
- Bakker, A., Fasano, J.B., Leng, D.E., 1994b. Pinpoint mixing problems with lasers and simulation software. *Chemical Engineering* 101, 94–100.
- Brucato, A., Ciofalo, M., Grisafi, F., Micale, G., 1998. Numerical prediction of flow field in baffled stirred vessels: a comparison of different modelling approaches. *Chemical Engineering Science* 53, 3653–3684.
- Brunazzi, E., Galletti, C., Paglianti, A., Pintus, S., 2003. Laser-Doppler measurements of turbulent flow parameters: comparison between baffled and unbaffled stirred tanks. *AIDIC Conference Series* 6, 67–76.
- Brunazzi, E., Galletti, C., Paglianti, A., Pintus, S., 2005. Screening tool to evaluate the levels of local anisotropy of turbulence in stirred vessels. *Industrial & Engineering Chemistry Research* 44, 5836–5844.
- Ciofalo, M., Brucato, A., Grisafi, F., Torraca, N., 1996. Turbulent flow in closed and free-surface unbaffled tanks stirred by radial impellers. *Chemical Engineering Science* 51, 3557–3573.
- Hall, J.F., Barigou, M., Simmons, M.J.H., Stitt, E.H., 2004. Mixing in unbaffled high-throughput experimental reactors. *Industrial & Engineering Chemistry Research* 43, 4149–4158.
- Hall, J.F., Barigou, M., Simmons, M.J.H., Stitt, E.H., 2005. Comparative study of different mixing strategies in small high throughput experimental reactors. *Chemical Engineering Science* 60, 2355–2368.
- Jones, R.M., Harvey III, A.D., Acharya, S., 2001. Two-equation turbulence modeling for impeller stirred Tanks. *Journal of Fluids Engineering* 123, 640–648.
- Joshi, J.B., Ranade, V.V., 2003. Computational fluid dynamics for designing process equipment: expectation, current status, and path forward. *Industrial & Engineering Chemical Research* 42, 1115–1128.
- Karcz, J., Cudak, M., Szoplik, J., 2005. Stirring of a liquid in a stirred tank with an eccentrically located impeller. *Chemical Engineering Science* 60, 2369–2380.
- Medek, J., Fort, I., 1985. Mixing in vessel with eccentric mixing. In: *Proceedings of the Fifth European Conference on Mixing*, Würzburg, West Germany, 10–12 June, BHRA, Cranfield, pp. 263–280.
- Montante, G., Lee, K.C., Brucato, A., Yianneskis, M., 2001. Numerical simulations of the dependency of flow pattern on impeller clearance in stirred vessels. *Chemical Engineering Science* 56, 3751–3770.
- Murthy, S.S., Jayanti, S., 2002. CFD study of power and mixing time for paddle mixing in unbaffled vessels. *Chemical Engineering Research & Design* 80, 482–498.
- Ng, K., Yianneskis, M., 2000. Observation on the distribution of energy dissipation in stirred vessels. *Chemical Engineering Research & Design* 78, 334–341.
- Nishikawa, M., Ashiwake, K., Hashimoto, S., 1979. Agitation power and mixing time in off-centring mixing. *International Chemical Engineering* 19, 153–159.
- Novak, V., Rieger, F., 1994. Mixing in unbaffled vessels. *ICHEME Symposium Series no. 136*, 511–518.
- Oshinowo, L., Jaworski, Z., Dyster, K.N., Marshall, E., Nienow, A.W., 2000. Predicting the tangential velocity field in stirred tanks using the Multiple Reference Frames (MRF) model with validation by LDA measurements. In: *Proceedings of 10th European Conference on Mixing*, Delft, 2–5 July, Amsterdam, pp. 281–288.
- Ranade, V.V., Joshi, J.B., Marathe, A.G., 1989. Flow generated by pitched blade turbine-II: simulation using $k-\epsilon$ model. *Chemical Engineering Communications* 81, 225–248.
- Rivera, C., Heniche, M., Ascanio, G., Tanguy, P., 2004. A virtual finite element model for centred and eccentric mixer configurations. *Computers and Chemical Engineering* 28, 2459–2468.
- Wegner, B., Maltsev, A., Schneider, C., Sadiki, A., Dreizler, A., Janicka, J., 2004. Assessment of unsteady RANS in predicting swirl flow instability based on LES and experiments. *International Journal of Heat and Fluid Flow* 25, 528–536.
- Yoon, H.S., Hill, D.F., Balachandar, S., Adrian, R.J., Ha, M.Y., 2005. Reynolds number scaling of flow in a Rushton turbine stirred tank. Part I. Mean flow, circular jet and tip vortex scaling. *Chemical Engineering Science* 60, 3169–3183.